Fluid Phase Equilibria 281 (2009) 49–59

Contents lists available at ScienceDirect

Fluid Phase Equilibria

journal homepage: www.elsevier.com/locate/fluid

Study of azeotropic mixtures with the advanced distillation curve approach☆

Amelia B. Hadler, Lisa S. Ott, Thomas J. Bruno*

Physical and Chemical Properties Division, National Institute of Standards and Technology, Boulder, CO, United States

ARTICLE INFO

Article history:
Received 27 January 2009
Received in revised form 30 March 2009
Accepted 3 April 2009
Available online 11 April 2009

Keywords:
Acetone + chloroform
Advanced distillation curve
Azeotrope
Ethanol + benzene
2-propanol + benzene
Phase equilibrium

ABSTRACT

Classical methods for the study of complex fluid phase behavior include static and dynamic equilibrium cells that usually require vapor and liquid recirculation. These are sophisticated, costly apparatus that require highly trained operators, usually months of labor-intensive work per mixture, and the data analysis is also rather complex. Simpler approaches to the fundamental study of azeotropes are highly desirable, even if they provide only selected cuts through the phase diagram. Recently, we introduced an advanced distillation curve measurement method featuring: (1) a composition explicit data channel for each distillate fraction (for both qualitative and quantitative analysis), (2) temperature measurements that are true thermodynamic state points that can be modeled with an equation of state, (3) temperature, volume and pressure measurements of low uncertainty suitable for equation of state development, (4) consistency with a century of historical data, (5) an assessment of the energy content of each distillate fraction, (6) trace chemical analysis of each distillate fraction, and (7) corrosivity assessment of each distillate fraction. We have applied this technique to the study of azeotropic mixtures, for which this method provides the bubble point temperature and dew point composition, completely defining the thermodynamic state from the Gibbs phase rule perspective. In this paper, we present the application of the approach to several simple binary azeotropic mixtures: ethanol + benzene, 2-propanol + benzene, and acetone + chloroform.
Published by Elsevier B.V.

1. Introduction

Azeotropic mixtures are among the most fascinating and at the same time the most complicated manifestations of phase equilibrium. They also play a critical role in many industrial processes (and the resulting products), especially separations [1,2]. With the current interest in alcohol based fuels (including those referred to as biofuels) alcohol extended fuels, and fuels oxygenated with alcohols for environmental reasons, the need to consider azeotropes in phase equilibrium is clear. Indeed, dealing with mixtures of hydrocarbons with lower alcohols means dealing with azeotropes.

Simply stated, an azeotrope is a mixture of two or more components that cannot be separated by simple distillation. This very simple definition conceals interesting thermodynamic details of fluid mixture non-ideality and the single point at which the liquid and vapor composition is the same [3,4]. Each mixture that forms an azeotrope has a characteristic composition, temperature and pressure at which the azeotrope exists. The boiling point of an azeotrope is either higher than its individual components (called a negative azeotrope) or lower than its individual components (called a positive azeotrope). This is most commonly presented in terms of the T–x diagram (where T is the temperature and x is the mole fraction of one constituent), a two-dimensional cut through the three dimensional (P–T–x, where P is the pressure) phase diagram in which there is the liquid region at the bottom of the chart (extending to the bubble point line), a two-phase region contained between the bubble and dew point lines, and finally the vapor region above the dew point line [5,6].

In terms of the mixture pressure, negative deviations from Raoult's Law resulting in a horizontal tangent on the P–x diagram will produce a negative (or high boiling) azeotrope, while positive deviations from Raoult's Law resulting in a horizontal tangent will produce a positive (or low boiling) azeotrope. The formation of azeotropes is a consequence of intermolecular interactions, and can be elucidated in terms of Raoult's Law. When a binary mixture of two fluids, a and b, form an ideal solution and obey Raoult's Law (producing a straight line trace on the T–x diagram), the interaction of a with a and b with b is essentially the same as the interaction between a and b. In this context, an interaction is considered a pairing that is longer lived than random pairing. When a and b have a strong mutual repulsion, positive deviations from Raoult's Law are observed, and the formation of a positive azeotrope (with a minimum in the boiling temperature) can result. The escaping tendency of the molecules from the condensed phase is magnified due to the intermolecular interactions. Thus the molecules "escape" the liquid with a decreased input of energy (as manifest in the temperature). When a and b have a strong attraction, negative deviations from

☆ Contribution of the United States government, not subject to copyright in the United States.

* Corresponding author. Tel.: +1 303 497 5158.
E-mail address: bruno@boulder.nist.gov (T.J. Bruno).

0378-3812/$ – see front matter. Published by Elsevier B.V.
doi:10.1016/j.fluid.2009.04.001

Raoult's Law are observed, with the potential of forming a negative azeotrope (with a maximum in the boiling temperature). The molecules require an increased input of energy to "escape" (therefore the higher temperature). In terms of total number of known azeotropic mixtures, the majority of fluid combinations form positive azeotropes.

Classical measurements of phase equilibrium, including measurements on azeotropes, are done with apparatus that dwell at individual state points of temperature, pressure and composition, and essentially generate a series of "snap shots" of the experimental variables [7–13]. In practice, one can use either a static or a dynamic approach. In the static approach, a mixture is prepared (usually as a liquid) that has a selected mole fraction, and is maintained in a closed vessel at a desired starting temperature and pressure. The temperature is increased until the bubble point is noted either visually or with instrumentation. Then, the mixture is heated until the entire cell content is vaporized, and the temperature is noted. Then the temperature is slowly decreased until the dew point is noted. Doing this experiment for multiple starting concentrations allows one to map out the T–x diagram. An alternative is the dynamic approach in which the composition of the fluid inside the cell is varied with one or more injection pumps, and the composition is measured along with the temperature and pressure. Composition is usually measured chromatographically, although in some cases this can be done spectroscopically. Liquid and vapor recirculation is frequently used with such apparatus to achieve equilibration. Such classical measurements are costly and time consuming, and require highly trained operators for the measurements and data reduction.

Alternative approaches, even if simplified, are highly desirable to these classical vapor liquid equilibrium (VLE) measurements. Indeed, in recent years the capability to measure VLE has declined in laboratories worldwide such that only a small number of apparatus are now available. This comes at a time of increasing interest in fuels that can be produced from renewable sources, including biomass. Lower alcohols (primarily ethanol) added to gasoline have long been used for environmental mitigation. Now, such fuels are viewed as an avenue to reduce dependence on imported petroleum based fuels, and this is reflected in government policy to increase fuel ethanol production. The admixture of ethanol with gasoline streams is not without technical difficulties, and doing so on an ever-increasing scale requires that such problems be addressed. A complication that can be very unfavorable is the formation of azeotropes in mixtures of lower alcohols (such as ethanol) with hydrocarbon components.

In recent work, we described a method and apparatus for an advanced distillation curve (ADC) measurement that is especially applicable to the characterization of fuels. The distillation curve is a graphical depiction of the boiling temperature of a fluid mixture plotted against the volume fraction distilled. This volume fraction is usually expressed as a cumulative percent of the total volume. The new method, called the advanced distillation curve method, is a significant improvement over current approaches, featuring (1) a composition explicit data channel for each distillate fraction (for both qualitative and quantitative analysis), (2) temperature measurements that are true thermodynamic state points that can be modeled with an equation of state, (3) temperature, volume and pressure measurements of low uncertainty suitable for equation of state development, (4) consistency with a century of historical data, (5) an assessment of the energy content of each distillate fraction, (6) trace chemical analysis of each distillate fraction, and (7) corrosivity assessment of each distillate fraction [14–29]. The method is rapid, with the complete distillation curve measurement taking approximately between 1 and 3 h, depending upon the fluid. We have applied this metrology to gasolines, aviation fuels, diesel fuels and rocket propellants. Clearly, it is not always needed or desirable to apply all aspects of the advanced distillation curve metrology in every application. For highly finished fuels such as gasoline, for example, it is usually unnecessary to assess corrosivity as a function of distillate fraction.

In terms of engineering requirements for complex fluids and fuels, the ADC provides many critical design and operational parameters. In terms of the T–x phase diagram, the data resulting from the ADC measurement consist of a measure of the bubble point temperature and the dew point composition. When compared to other VLE measurement techniques, this initially appears to provide two pieces of a four-piece puzzle (with the dew point temperature and the bubble point composition missing). In terms of the phase rule, however, the thermodynamic state is completely defined by the measurements of the ADC. The demonstrated ability to model the ADC results with the most modern and precise equations of state allows for an approximation of the phase diagram in a fraction of the time, and at a fraction of the cost, when compared with either a static or dynamic VLE instrument [30]. Moreover, we show here that the approach is particularly useful as applied to azeotropic mixtures.

In terms of a distillation experiment, the behavior of positive and negative azeotropes is fundamentally different. For a positive azeotrope (with a temperature minimum) removed from the azeotropic composition, distillation results in a vapor phase that

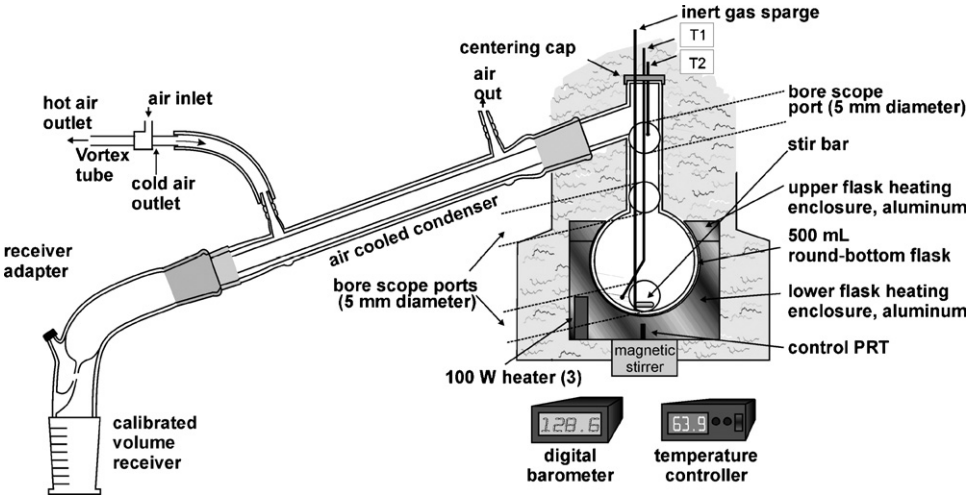

Fig. 1. Schematic diagram of the overall apparatus used for the measurement of distillation curves.

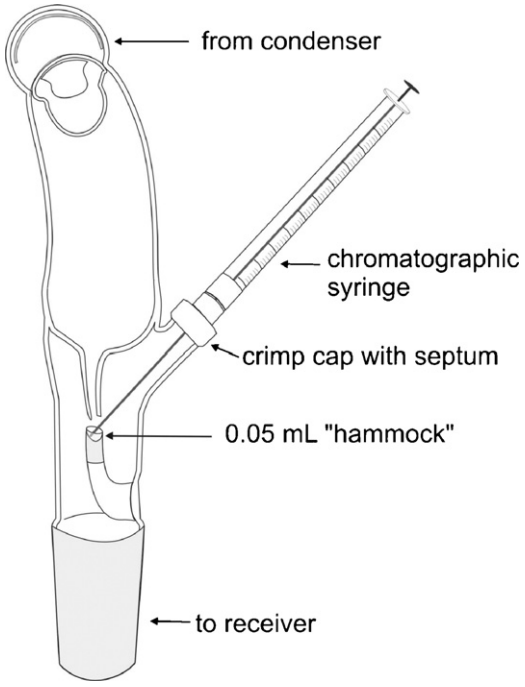

Fig. 2. Schematic diagram of the receiver adapter to provide on-the-fly sampling of distillate cuts for subsequent analysis.

approaches the azeotropic composition, while the fluid remaining in the distillation flask approaches one or the other of the pure components. For a negative azeotrope (with a temperature maximum) removed from the azeotropic composition, distillation results in a vapor phase that approaches one or the other of the pure components, while the fluid remaining in the distillation flask approaches the azeotropic composition.

The apparatus and procedure for the measurement of the composition ADC have been discussed in detail elsewhere, only a brief description will be provided here. The apparatus is depicted schematically in Fig. 1, with additional details provided in Figs. 2 and 3. The stirred distillation flask is placed in an aluminium heating jacket contoured to fit the flask. The jacket is resistively heated, controlled by a model predictive PID controller that applies a precise thermal profile to the fluid. Three observation ports are provided in the insulation to allow penetration with a flexible, illuminated bore scope. The ports are placed to observe the fluid in the boiling flask, the top of the boiling flask (where the spherical section joins the head), and the distillation head (at the bottom of the take-off).

Above the distillation flask, a centering adapter provides access for two thermally tempered, calibrated thermocouples that enter the distillation head. One thermocouple (TC1) is submerged in the fluid and the other (TC2) is centered at the low point of distillate take-off. Also in the head is an inert gas blanket for use with thermally unstable fluids. Distillate is taken off the flask with a distillation head, into a forced-air condenser chilled with a vortex tube. Following the condenser, the distillate enters a new transfer adapter that allows instantaneous sampling of distillate for analysis. When the sample leaves the adapter, it flows into the calibrated, level-stabilized receiver for a precise volume measurement. The atmospheric pressure is measured with an electronic strain gauge barometer, and in some cases the fluid transit time is measured with an electronic timer.

To measure a distillation curve, fluid (40–200 mL) is placed in the distillation flask and the heating profile begins. The profile typically has the sigmoidal shape of a distillation curve, but continuously leads the fluid by ≈20 °C. For each ADC measurement, we can record

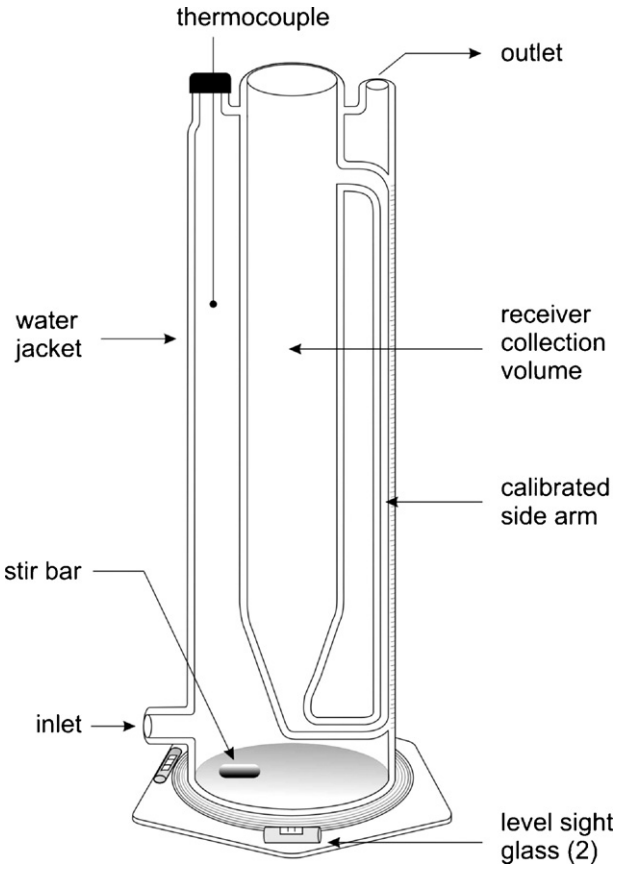

Fig. 3. Schematic diagram of the level-stabilized receiver for distillation curve measurement.

a data grid consisting of: T_k, the temperature measured in the fluid (with TC1), T_h, the temperature in the head (measured with TC2), the corresponding fluid volume, the elapsed time, and the external (atmospheric) pressure. Both of these temperatures are important, since T_k is a true thermodynamic state point while T_h provides consistency with historical data (which in many cases spans a century). When needed, the transit time (or volume flow rate) is also measured for each fraction. This is most often done if the data are to be used for equation of state development, where the assumption of constant mass flow must be valid in the model and in the experiment [31,32]. Along with these data, one withdraws a fluid sample of each fraction for detailed analysis. While this procedure provides access to the detailed composition, energy content, corrosivity, etc., corresponding to each datum in the grid, our purpose in this paper is to describe specifically the application to azeotropic mixtures.

In a typical measurement of a complex, multicomponent fluid, the T_k measurement is higher than the T_h measurement by several (5–15) degrees. This must be the case, since the mass transfer driving force comes from the temperature differential between the kettle and the head. Indeed, it is this driving force that causes the composition to change during the distillation. Moreover, the curve is typically a subtle sigmoid or growth curve, increasing in temperature from the early fractions to the late fractions. If one performs an ADC measurement on a pure fluid, the temperature difference between T_k and T_h is very small, no more than 0.1 °C; the composition is not changing during the distillation. Moreover, the curve for a pure fluid is flat with no slope [17]. We would expect this difference in temperature differential and slope to be reflected in the distillation of an azeotrope, since it behaves like a pure fluid. Mixtures of gasoline oxygenates in fact show this behavior, since the lower alcohols form azeotropes with many of the hydrocarbon components in gasoline [26]. In Fig. 4a, we show the distillation curves

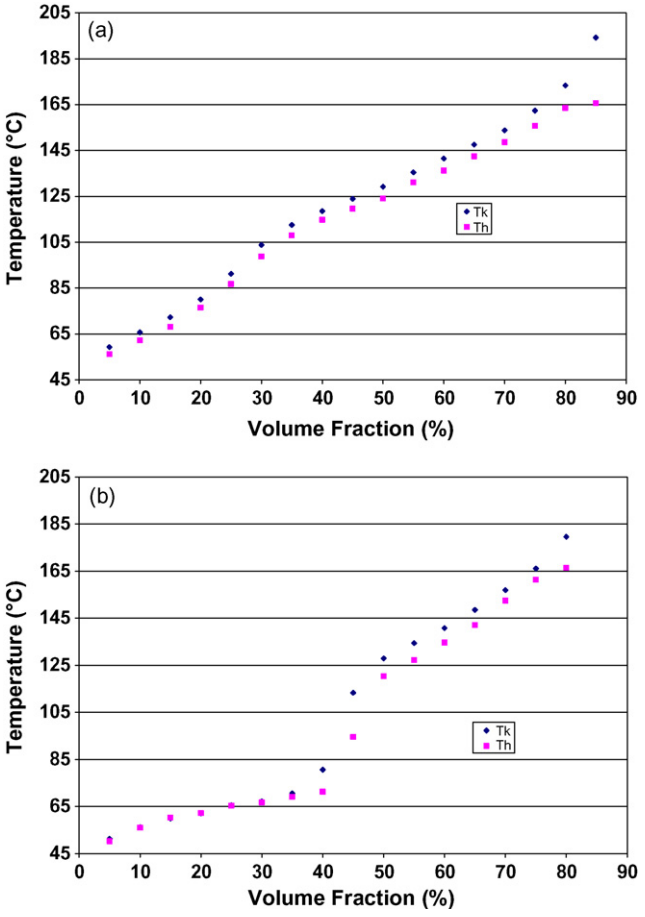

Fig. 4. (a) Distillation curves of 91 AI gasoline, presented in terms of T_k and T_h. The average difference in T_k and T_h is 6.2 °C. (b) Distillation curves of 91 AI gasoline + 15% methanol, presented in terms of T_k and T_h. One notes both the azeotropic inflection and temperature convergence from 0% to 35% distillate volume fraction.

of a 91 AI (antiknock index) premium, winter grade gasoline, presented in T_k and T_h. This fuel has no added oxygenate. We note for this complex, multi-component fluid that T_k is always higher than T_h by an average of 6.2 °C. In Fig. 4b we show the same gasoline with 15% (v/v) methanol. Two features are noteworthy. First we note a flattening of the curve for distillate volume fractions up to approximately 40%, relative to that for the straight gasoline. We call this the azeotropic inflection, caused by the liquid and vapor phases approaching the same composition due to the formation of azeotropic mixtures. This persists until the methanol has been distilled out of the mixture. Second, we also note the convergence of T_k and T_h in this region, which we have called the azeotropic convergence. Here, the difference between T_k and T_h averages 0.3 °C, while subsequent to the azeotropic inflection, the difference increases to an average of 8.6 °C. We also note that for mixtures in which the component boiling points are close, the difference between T_k and T_h is far less pronounced. We mention in passing an additional multi-component mixture in which the azeotropic inflection and convergence were important in the interpretation of the distillation curve results. In our recent measurements of gasoline with biobutanol (mixtures of gasoline + *n*-butanol, gasoline + 2-butanol, gasoline + iso-butanol and gasoline + *t*-butanol), we noted similar behavior [33].

To demonstrate the potential of the method in helping us to fundamentally understand the phase equilibrium of azeotropic mixtures, we present measurements on several well-known mixtures: ethanol + benzene, 2-propanol + benzene and acetone + chloroform. We stress that our purpose in this work is not to shed additional light on these very well studied and understood mixtures. Rather, our purpose here is to illustrate the response and utility of the ADC approach in the rapid identification and fundamental study of azeotropic mixtures. We will devote considerable time to the discussion of the features of the ethanol + benzene series of mixtures, and far less to the other two, because many of the features are common to all mixtures. For 2-propanol + benzene and acetone + chloroform, we will concentrate on the differences with the ethanol + benzene binary.

2. Experimental

The ethanol, benzene, chloroform, acetone and 2-propanol used in this work were all obtained from commercial sources. The fluids were analyzed by gas chromatography (30 m capillary column of 5% phenyl–95% dimethyl polysiloxane having a thickness of 1 μm, temperature program from 50 to 170 °C, 5 °C/min) using flame ionization detection and mass spectrometric detection [34,35]. These analyses revealed the purities of each fluid to be approximately 99.9% or higher, and each fluid was used without further purification. All fluids were handled in a fume hood to minimize operator exposure to vapors, and they were kept in sealed containers to minimize the uptake of water. The *n*-dodecane that was used as a solvent in this work was of similar purity which was also verified as noted above.

The apparatus and procedure of the advanced distillation curve measurement have been presented in several sources (see the earlier references), so only the essential details will be presented here. The distillation flask was a 500 mL round bottom flask that was placed in a two-part aluminium heating jacket, the lower part of which was contoured to fit the flask. Above the distillation flask, a centering adapter provided access for two thermally tempered J-type thermocouples that enter the distillation head. One thermocouple enters the distillation flask and is submerged in the fluid, to monitor the temperature of the bulk fluid, T_k. This provides the thermodynamic state point temperature of the fluid. The other thermocouple is centered at the low point of distillate take-off, to monitor T_h. Both of the thermocouples were calibrated in an indium triple point cell traceable to a NIST standard. A minor difference in the apparatus specific to this work is the removal of much of the insulation that normally surrounds the distillation head in the ADC apparatus. We have found that when dealing with fluids that boil at relatively low temperatures (such as the binaries in this work, or some volatile gasoline samples), we often observe instrumental anomalies in which T_h begins to lead T_k. This occurs when heat is more efficiently transferred by the glass of the apparatus, radiatively heating the T_h thermocouple, whereas, normally the vaporized fluid heats this thermocouple. Removal of some insulation easily remedies this problem, although we have found with fluids that boil at lower temperatures than those studied here (that is, in the range of 50–60 °C), we often need to cool the head with a small muffin fan to minimize the radiative heat transfer from the walls. We note that for the binaries studied in this work, there is no need for historical consistency because the *T*–*x* diagrams that are available were measured with VLE instrumentation, not distillation instrumentation. Moreover, the component boiling temperatures are always relatively close to one another. Thus, the only purpose in measuring T_h is as a diagnostic for the avoidance of the heat transfer anomaly discussed above.

The estimated uncertainty (with a coverage factor $k = 2$) in the measured temperatures was 0.5 °C. We note that the experimental uncertainty of T_k is always somewhat lower than that of T_h, but as a conservative position, we use the higher value for both temperatures. The uncertainty in the volume measurement that was used to obtain the distillate volume fraction was 0.05 mL in each case. The uncertainty in the pressure measurement (assessed by

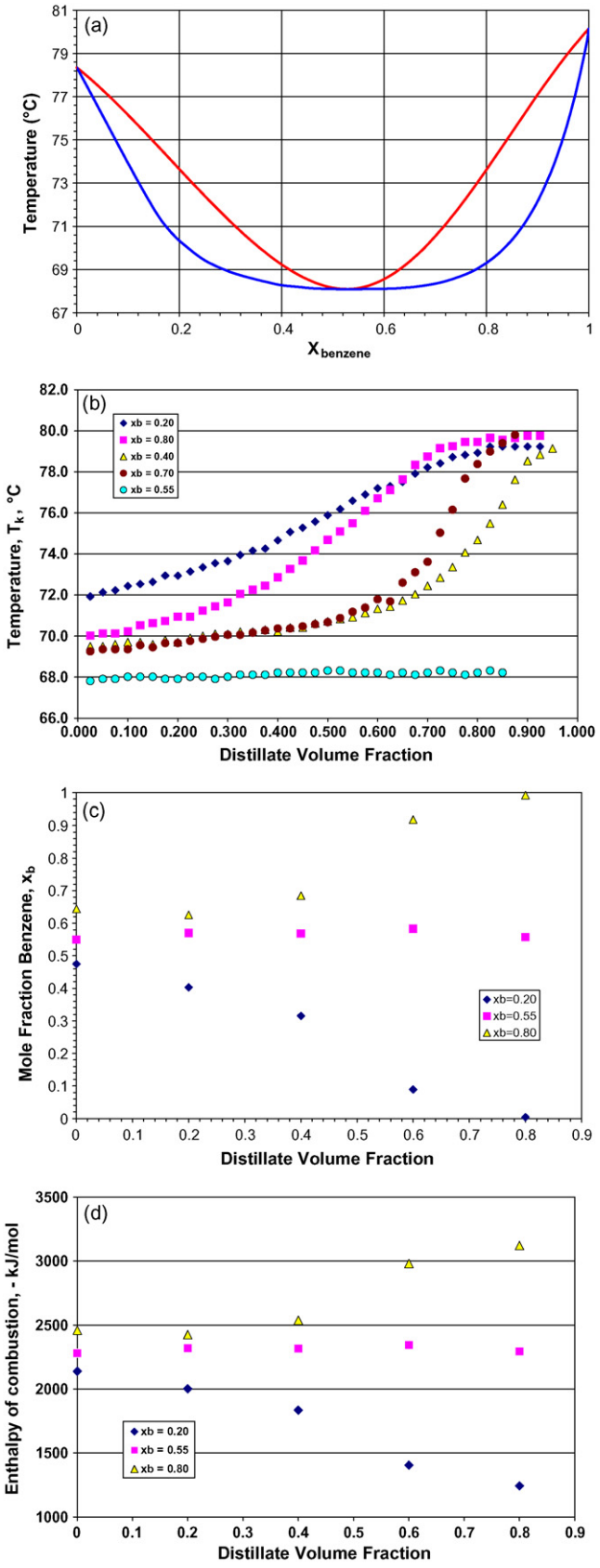

Fig. 5. (a) A *T*–*x* phase diagram for the ethanol + benzene binary mixture showing the minimum boiling positive (minimum vapor pressure) azeotrope. (b) A plot of the distillation curve data for binary mixtures of ethanol + benzene at benzene mole fractions x_b = 0.20, 0.40, 0.55, 0.70 and 0.80. The uncertainty is discussed in the text. (c) The results of the gas chromatographic analysis of distillate fractions from the starting mixtures of ethanol + benzene at mole fractions x_b = 0.20, 0.55 and 0.80. The uncertainty bars are smaller than the plotting symbols. Note that the points that coincide with the left vertical axis are at a distillate fraction of 0.00025 (0.025%). (d) The enthalpy of combustion as a function of distillate fraction for the ethanol + benzene mixtures presented in (c). The uncertainty is discussed in the text.

automatically logging a pressure measurement every 15 s for the duration of a typical distillation) was 0.001 kPa. The relatively low uncertainties in the measured quantities in the advanced distillation curve approach facilitate modeling the results, for example, with an equation of state.

Since the measurements of the distillation curves were performed at ambient atmospheric pressure (measured with an electronic barometer), temperature readings were corrected for what should be obtained at standard atmospheric pressure. This was done with the modified Sydney Young equation, in which the constant term was assigned values consistent with Young's compilation [36–38]. Uncertainty in the adjustment that results from application of the Sydney Young equation can be several degrees, depending upon the slope of distillation curve (that is, how rapidly the temperatures change in response to the changing composition) [39]. We use the Sydney Young equation because the VLE measurements on the mixtures we have studied were made at atmospheric pressure, and a comparison can only be made if the temperatures are adjusted to account for our elevation.

The other major features of the apparatus, including the level-stabilized receiver, the sampling adapter, the model predictive temperature controller, and the vortex tube chilling of the condenser (to 5 °C), are unchanged from previous reports. In this work, we used 200 mL aliquots of fluid mixture for each measurement. Mixtures were prepared on a molar basis by combining the appropriate mass of fluid in stoppered mixing cylinders.

3. Results and discussion

3.1. Ethanol + benzene

One of the most well-known minimum boiling binary azeotrope is that formed by benzene and ethanol [40–42]. It is often presented in introductory texts as an instructional example because of the striking features and structure of the phase diagram (the temperature differences are significant, the two-phase region is large, and the azeotrope occurs nearly at the midpoint of the *T*–*x* diagram) [5,6]. This mixture is also industrially important in the formulation and design of oxygenated and reformulated gasolines [43]. The *T*–*x* phase diagram of this binary, shown in Fig. 5a, is anchored on the left side by the pure ethanol point (at a normal boiling temperature of 78.4 °C), and on the right side by the pure benzene point (at a normal boiling temperature of 80.1 °C). The bubble and dew point curves meet at the minimum located at 68.2 °C. Centered about the minimum on the bubble point curve is a relatively flat region where the slopes in either direction are gentle. These slopes become increasingly more pronounced as one proceeds away from the azeotrope. The dew point curves proceed from the azeotropic point to the pure component points in a more linear fashion with relatively constant slope.

We have measured the distillation behavior for binary mixtures of ethanol + benzene with starting compositions of 0.20, 0.40, 0.55, 0.70 and 0.80 mole fraction of benzene (x_b). These mixtures were prepared gravimetrically in stoppered mixing cylinders, and had an uncertainty in mole fraction of 0.01. During the initial heating of each sample in the distillation flask, the behavior of the fluid was observed. Direct observation through the flask window or through the illuminated bore scope allowed measurement of the onset of boiling for each of the mixtures. Typically, during the early stages of a measurement the first bubbles will appear intermittently, and

Table 1
The initial boiling behavior (presented in °C) of binary mixtures of ethanol + benzene with starting compositions of 0.20, 0.40, 0.55, 0.70 and 0.80 mole fraction of benzene (denoted as x_b in the table). The vapor rising temperatures are the initial boiling temperatures for the mixture. In each case, the experimental pressure is provided, although the temperatures presented in the table have been adjusted with the Sydney Young equation to approximate what would be obtained at standard atmospheric pressure.

	$x_b = 0.20$	$x_b = 0.40$	$x_b = 0.55$	$x_b = 0.70$	$x_b = 0.80$
Vapor rising temperature (IBT) (°C)	71.7	69.5	67.8	69.2	69.8
Ambient atmospheric pressure (kPa)	83.8	83.4	83.3	83.6	83.7

this action will quell if the stirrer is stopped momentarily. Sustained vapor bubbling is then observed. In the context of the advanced distillation curve measurement, sustained bubbling is also somewhat intermittent, but it is observable even with the stirrer is momentarily stopped. Most importantly, the temperature at which vapor is first observed to rise into the distillation head is observed. This is termed the vapor rise temperature. These observations are important especially with complex fluids because they are the initial boiling temperatures (IBT) of each fluid. The uncertainty in the vapor rise temperature is approximately 0.2 °C.

The initial boiling behaviors of the five binary mixtures of ethanol + benzene are summarized in Table 1. These measurements have been made at the ambient pressures listed in the table (at an elevation of 1655 m in Boulder, CO), and adjusted to the predicted result for atmospheric pressure with the Sydney Young equation, as discussed above. We note that the initial temperatures are consistent with the trends represented on the *T*–*x* diagram, but a slight offset is observed because of the application of the Sydney Young equation. The original *T*–*x* diagram in Fig. 5a was measured near sea level (with an approximate atmospheric pressure of 101 kPa) [40,41]. This is not a serious disadvantage because with the measured atmospheric pressure (provided in the table), the actual measured temperature is recovered easily. This would in fact be necessary for any equation of state development; we chose to present adjusted temperatures simply to be consistent with the phase diagram and a century of distillation curve practice.

For the $x_b = 0.20$ mixture, we note that the initial boiling temperature is relatively high, at 71.7 °C, since the bubble point of this mixture is on the relatively steep side of the *T*–*x* diagram. For the mixtures at $x_b = 0.40$, 0.55, and 0.70, the bubble point line on the *T*–*x* diagram is relatively flat, and we note that the initial boiling temperatures are correspondingly consistent, varying only by 0.3 °C. The $x_b = 0.80$ mixture is located on the upward part of the bubble point line on the right side of the *T*–*x* diagram, and thus we note a corresponding increase in the initial boiling temperature.

In Table 2 and Fig. 5b, we present results from the ADC measurement of the five binary mixtures of ethanol + benzene mixtures discussed above. For brevity, in the table we list only volume fraction increments of 0.05, while in the figure all data collected are shown. The shapes of the curves for the mixtures $x_b = 0.20, 0.40, 0.70$ and 0.80 are pronounced sigmoids, consistent with what is typically observed for binary mixtures of components with distinct physical properties. The curve for $x_b = 0.55$ is essentially a straight line with no slope. This is the typical distillation curve that is observed when a pure fluid is measured; this was demonstrated with the measurement of the missile fuel, JP-10 [17]. In the present case, the $x_b = 0.55$ curve is not for a pure fluid, but rather for a binary mixture at the azeotropic composition. We can therefore represent the temperature as a mean of all temperatures along this line: 68.1 °C with an uncertainty of 0.1 °C. This compares very well with the literature value of the azeotropic temperature of 68.2 °C, and shows how the ADC can be used to determine the azeotropic state point.

We note that the distillation curves for the starting compositions $x_b = 0.20$ and 0.40 converge at a temperature of 78.9 °C, while those at $x_b = 0.70$ and 0.80 converge at a temperature of 80.9 °C. These two different families of curves, which begin with starting compositions on either side of the azeotrope, converge to the appropriate pure component, 78.9 °C (for $x_b = 0.20$ and 0.40, converging to ethanol) and 80.9 (for $x_b = 0.70$ and 0.80 converging to benzene). We note that our measured temperatures are somewhat displaced from the accepted pure component boiling temperatures again because of our elevation and the inherent uncertainty in the Sydney Young adjustment. Moreover, we have carried out the distillation only to a distillate volume fraction of approximately 95%; beyond this volume fraction, we encounter thermocouple lift out, and we are no longer able to measure a fluid temperature.

We note that the shapes of the curves for $x_b = 0.20$ and 0.80 are initially far steeper than those for $x_b = 0.40$ and 0.70. This can be explained with reference to the *T*–*x* diagram. We note that the initial steepness of slope corresponds with the pronounced increase in slope of the bubble point curve. Where the *T*–*x* diagram is steep, the distillation curve is correspondingly steep. The curves for $x_b = 0.40$ and 0.70 ultimately become very steep as the composition changes during the distillation. Clearly, on either side of the azeotropic composition, one must eventually arrive at the appropriate pure component.

Table 2
Distillation curve data (presented in °C) for binary mixtures of ethanol + benzene at benzene mole fractions of 0.20, 0.40, 0.55, 0.70 and 0.80. In each case, the experimental pressure is provided, although the temperatures presented in the table have been adjusted with the Sydney Young equation to approximate what would be obtained at standard atmospheric pressure.

Distillate volume fraction	$x_b = 0.20$, 83.8 kPa T_k	$x_b = 0.40$, 83.4 kPa T_k	$x_b = 0.55$, 83.3 kPa T_k	$x_b = 0.70$, 83.6 kPa T_k	$x_b = 0.80$, 83.7 kPa T_k
0.05	72.1	69.5	67.9	69.4	70.1
0.10	72.4	69.7	68.0	69.4	70.2
0.15	72.6	69.6	68.0	69.5	70.6
0.20	72.9	69.7	67.9	69.7	70.9
0.25	73.3	70.0	68.0	69.9	71.2
0.30	73.7	70.1	68.0	70.1	71.6
0.35	74.2	70.2	68.1	70.2	72.3
0.40	74.7	70.2	68.2	70.4	72.9
0.45	75.3	70.4	68.2	70.5	73.7
0.50	75.9	70.7	68.2	70.7	74.7
0.55	76.6	70.9	68.2	71.2	75.5
0.60	77.2	71.3	68.2	71.8	76.7
0.65	77.5	71.7	68.2	72.6	77.6
0.70	78.2	72.4	68.2	73.6	78.7
0.75	78.7	73.4	68.2	76.2	79.3
0.80	78.9	74.7	68.2	78.4	79.5

We can now examine the results from the composition explicit data channel, in which we have access to the dew point compositions. Aliquots of 7 μL of distillate were sampled with a blunt tipped chromatographic syringe from the sampling hammock of the receiver adapter. Samples were taken for distillate volume fractions of 0.025, 0.2, 0.4, 0.6, and 0.8, the sample at a fraction of 0.025 being the first drop of distillate to emerge from the instrument. The aliquots were added to a vial containing a known mass of solvent (*n*-dodecane), and analyzed by gas chromatography (30 m capillary column, 0.250 mm outside diameter, coated with 1 μm of dimethyl polysiloxane, temperature programmed from 90 to 250 °C at 8 °C/min, autosampler injection into a split injector set at 100:1, flame ionization detection). This particular solvent was chosen to provide no interference with the chromatographic peaks of interest, and also to serve as a "keeper" that would minimize any evaporative loss of solute. Calibration was provided by external standards (comprised of four mixtures of each binary) measured on the chromatograph before and after each solution cut.

The results of the analysis of starting mixtures of $x_b = 0.20$, 0.55 and 0.80 are shown in Fig. 5c. One can see that the mixture with the azeotropic composition of $x_b = 0.55$ shows linear behavior with distillate fraction, with zero slope within experimental uncertainty. This mixture, when distilled, yields the expected constant composition. Our measured mole fractions (chromatographically measured at $x_b = 0.57$ with an uncertainty of 0.02, with a coverage factor $k = 2$), statistically, can only be represented by a mean. This is within the combined experimental uncertainty of the chromatographic result and that of the gravimetrically prepared starting mixture.

We note that the mixture prepared as $x_b = 0.20$ begins to distill (at a distillate fraction of 0.025) at a composition of $x_b = 0.47$. This composition of the dew point line is consistent with the *T*–*x* phase diagram of Fig. 5a; the vapor is enriched in benzene as the liquid becomes pure ethanol. We see that subsequent fractions of this mixture have progressively lower mole fractions of benzene, because progressively less benzene is available in the liquid to distill out. Ultimately, very little benzene is found at the distillate volume fraction of 0.8 (measured at $x_b = 0.004$), as the mixture left in the kettle becomes pure ethanol. When we begin on the other side of the azeotrope, at a starting mixture of $x_b = 0.80$, we see that the first drop to distill (again at a distillate fraction of 0.025) emerges with $x_b = 0.64$. This is also consistent with the phase diagram, since we expect the vapor composition along the dew point curve to show that the liquid remaining in the kettle is being depleted in ethanol as compared to the starting mixture. This is because the remaining liquid is becoming progressively richer in benzene. Ultimately, at a distillate volume fraction of 0.8, the distillate is indeed very rich in benzene, with $x_b = 0.99$. We note that although our measured compositions and temperatures are very close to what is expected from the phase diagram in each case, there is not an exact correspondence because the phase diagram was measured at approximately 101 kPa and our distillation curves were measured at approximately 83 kPa. The Sydney Young equation adjustment can account for some of this difference, but not all. As was mentioned earlier, this is of no real importance, since to use the data for equation of state development (in order to ultimately calculate the phase diagram), one would not use the Sydney Young adjustment at all [39].

In addition to the compositions and temperatures, we can use the composition channel of the ADC to obtain other intensive properties. We have shown, for example, that it is possible to calculate the composite enthalpy of combustion as a function of distillate fraction, neglecting the small contribution of the enthalpy of mixing [21]. This is relevant to the binary of ethanol + benzene because of its importance to reformulated fuels and biofuels. Following the procedure outlined, we present the composite enthalpy of combustion for each of the mixtures in Fig. 5d as an illustration. The uncertainties of these enthalpy values are less than 3. As expected, the azeotrope is nearly constant in energy content on a molar basis, while the mixture that approaches pure benzene increases in energy content, and that approaching pure ethanol decreases. As we have discussed elsewhere, it is often a more practical measure to discuss energy content of a fuel on a volume basis, and a conversion can be easily accomplished with either mixture density measurements or a correlation. While we have demonstrated that this information is useful when designing or specifying a mixture for use as a fuel, other enthalpic properties are accessible as a function of distillate fraction in this way. Spectroscopic determinations of association constant and enthalpy of association, for example, can be especially informative when studying azeotropic mixtures.

Table 3
The initial boiling behavior (presented in °C) of binary mixtures of 2-propanol + benzene with starting compositions of 0.20, 0.65 and 0.80 mole fraction of benzene (denoted as x_b in the table). The vapor rising temperatures are the initial boiling temperatures for the mixture. In each case, the experimental pressure is provided, although the temperatures presented in the table have been adjusted with the Sydney Young equation to approximate what would be obtained at standard atmospheric pressure.

	$x_b = 0.20$	$x_b = 0.61$	$x_b = 0.80$
Vapor rise temperature (IBT) (°C)	75.3	71.6	72.1
Observed pressure (kPa)	83.0	83.6	83.2

3.2. 2-Propanol + benzene

Another example of a positive azeotrope is the 2-propanol + benzene binary mixture, for which we have measured initial mixture compositions of 0.20, 0.61, and 0.80 mole fraction of benzene. The initial boiling behavior is summarized in Table 3, representative distillation curve data are provided in Table 4, and the curves are shown in Fig. 6a. The azeotrope occurs at $x_b = 0.61$. The *T*–*x* diagram of this binary (not shown) is similar to that of ethanol benzene, however in this case the anchor point of the 2-butanol is higher than that of benzene, at a normal boiling point of 82.5 °C. We note that the trends of the distillation curves are now reversed in the later stages; the curve terminating at pure 2-propanol reaches a higher temperature than the one terminating in pure benzene, while the azeotropic mixture at $x_b = 0.61$ is flat at an average temperature of 71.9 °C with an uncertainty of 0.1 °C. We note that this is the same as the literature value for this

Table 4
Distillation curve data (presented in °C) for binary mixtures of 2-propanol + benzene at benzene mole fractions of 0.20, 0.65, and 0.80. In each case, the experimental pressure is provided, although the temperatures presented in the table have been adjusted with the Sydney Young equation to approximate what would be obtained at standard atmospheric pressure.

Distillate volume fraction	$x_b = 0.20$, 83.0 kPa	$x_b = 0.65$, 83.6 kPa	$x_b = 0.80$, 83.2 kPa
0.05	75.9	71.7	72.5
0.10	76.1	71.7	72.6
0.15	76.6	71.7	72.8
0.20	77.1	71.8	72.9
0.25	77.8	71.8	73.2
0.30	78.3	71.9	73.4
0.35	79.0	72.0	73.8
0.40	79.7	71.9	74.3
0.45	80.8	72.1	74.8
0.50	81.7	72.0	75.7
0.55	82.4	72.1	76.7
0.60	82.9	72.0	77.9
0.65	83.1	72.0	79.0
0.70	83.1	71.9	79.6
0.75	83.1	71.9	80.1
0.80	82.9	71.9	80.1
0.85		71.8	80.0
0.90		71.7	

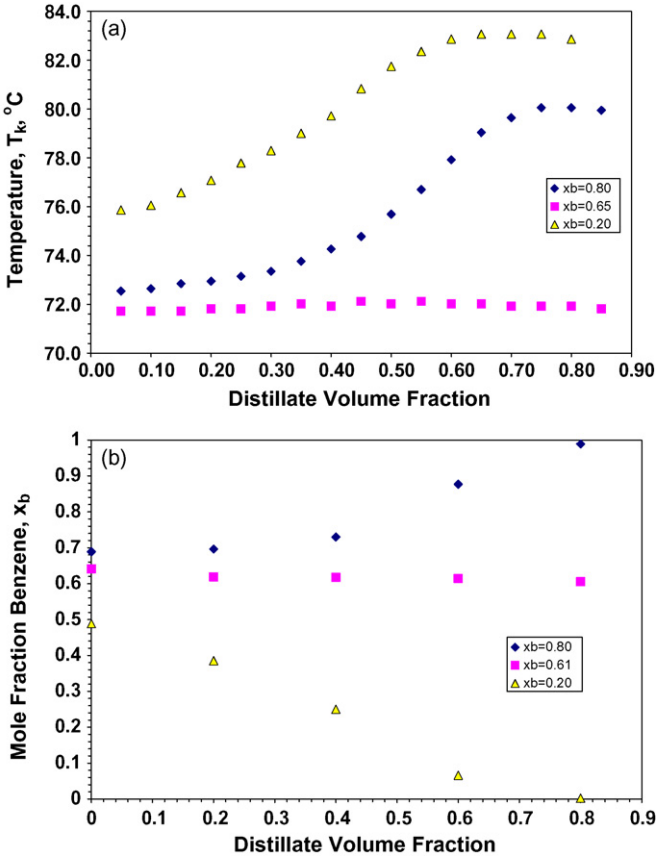

Fig. 6. (a) A plot of the distillation curve data for binary mixtures of 2-propanol + benzene at benzene mole fractions of 0.20, 0.65 and 0.80. The uncertainty is discussed in the text. (b) The results of the gas chromatographic analysis of distillate fractions from the starting mixtures of 2-propanol + benzene at $x_b = 0.20$, 0.61 and 0.80. The uncertainty bars are smaller than the plotting symbols. Note that the points that coincide with the left vertical axis are at a distillate fraction of 0.00025 (0.025%).

azeotropic state point [40,41,44]. The curve for $x_b = 0.80$ converges to a temperature of 80.1 °C (pure benzene), while the $x_b = 0.20$ curve converges to 83.0 °C (pure 2-propanol).

The results from the composition explicit data channel (measured similarly to that of ethanol + benzene), are shown in Fig. 6b, and we note a consistency with the distillation curves. First, we note that the measured composition of the azeotrope line is constant and can be best represented by a mean of $x_b = 0.62$ with an uncertainty of 0.01, which is within the experimental uncertainty of the literature value of the composition ($x_b = 0.61$). The measured compositions of the 0.025 distillate volume fractions of the $x_b = 0.20$ and 0.80 are not at the starting mole fractions of the mixtures, but we note that they are immediately shifted to the compositions of the dew point line. This is the behavior expected from the *T*–*x* diagram. Thereafter, there is a progression to the pure fluid, as with the ethanol + benzene binary.

We note that the behavior discussed above is easily distinguishable from mixtures that are zeotropic. For zeotropic mixtures, for any starting composition, the distillation temperature will gradually approach that of the less volatile component [14]. The gradual approach is indicative of small deviations from Raoult's law.

3.3. Acetone + chloroform

Negative azeotropes are far less common than positive azeotropes, and are therefore more difficult to study. It is simply more difficult to find a mixture that is amenable to a particular

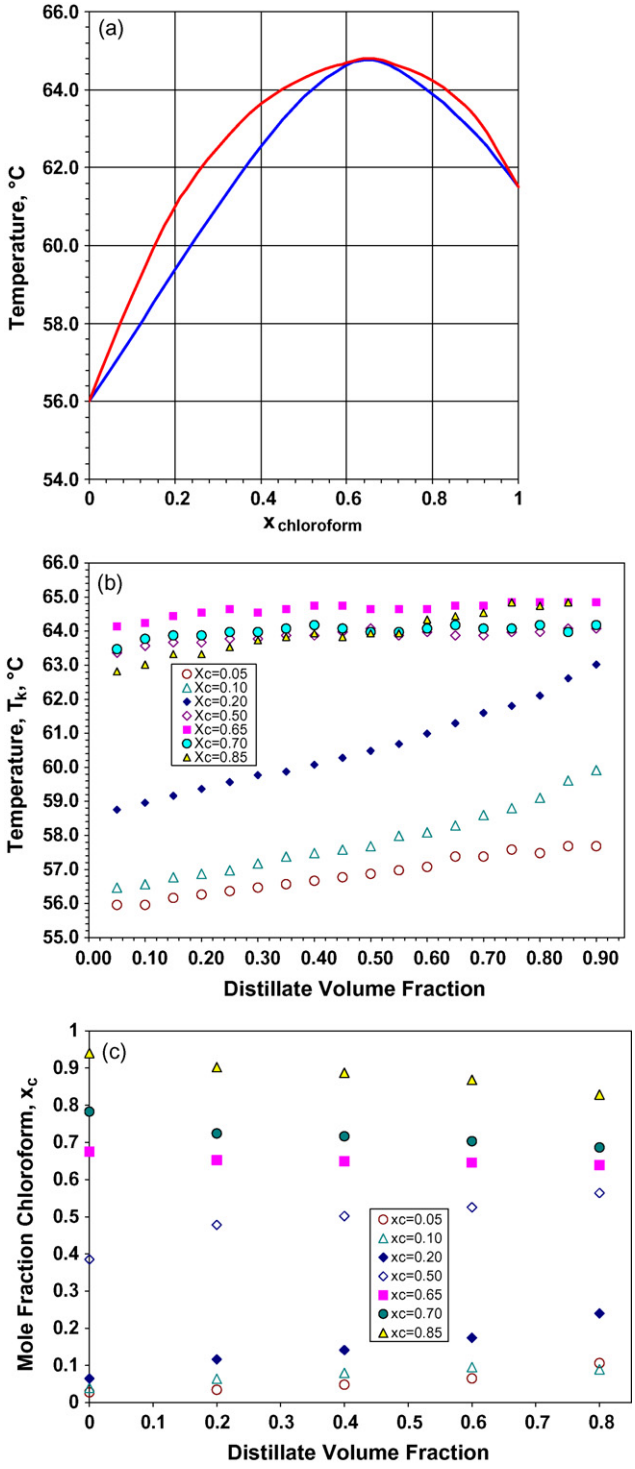

Fig. 7. (a) A *T*–*x* diagram for the mixture acetone + chloroform, showing the maximum boiling negative (minimum vapor pressure) azeotrope. (b) A plot of the distillation curve data for binary mixtures of acetone + chloroform at chloroform mole fractions of 0.05, 0.10, 0.20, 0.50, 0.65, 0.70, and 0.85. The uncertainty is discussed in the text. (c) The results of the gas chromatographic analysis of distillate fractions from the starting mixtures of acetone + chloroform at $x_c = 0.05$, 0.10, 0.20, 0.50, 0.65, 0.70, and 0.85. The uncertainty bars are smaller than the plotting symbols. Note that the points that coincide with the left vertical axis are at a distillate fraction of 0.00025 (0.025%).

metrology. A well-known example of a negative azeotropic binary mixture is the acetone + chloroform mixture, the *T*–*x* diagram for which is presented in Fig. 7a. The diagram is anchored on the left side by the pure acetone point (at a normal boiling temperature

Table 5
The initial boiling behavior (presented in °C) of binary mixtures of acetone + chloroform with starting compositions of 0.05, 0.10, 0.20, 0.50, 0.65, 0.70, and 0.85 mole fraction of chloroform (denoted as x_c in the table). The vapor rising temperatures are the initial boiling temperatures for the mixture. In each case, the experimental pressure is provided, although the temperatures presented in the table have been adjusted with the Sydney Young equation to approximate what would be obtained at standard atmospheric pressure.

	$x_c = 0.05$	$x_c = 0.10$	$x_c = 0.20$	$x_c = 0.50$	$x_c = 0.65$	$x_c = 0.70$	$x_c = 0.85$
Vapor rise temperature (IBT) (°C)	56.9	56.9	60.2	61.1	63.8	63.9	60.0
Observed pressure (kPa)	81.3	81.1	83.2	83.1	83.9	83.4	84.0

of 56.5 °C), and on the right side by the pure chloroform point (at a normal boiling temperature of 61.2 °C). The bubble and dew point curves meet at the maximum located at 64.7 °C. The negative azeotrope differs from the positive in that distillation of starting mixtures on either side of the maximum produces a mixture composition that approaches the azeotropic composition, rather than one of the pure components. For this binary, we have used the ADC to measure the distillation behavior of starting compositions of $x_c = 0.05$, 0.10, 0.20, 0.50, 0.65, 0.70, and 0.85, where x_c refers to the mole fraction of chloroform. The initial boiling behavior is summarized in Table 5, representative distillation curve data are provided in Table 6, and the curves are shown in Fig. 7b.

We first note that the initial temperatures are consistent with the trends represented on the *T–x* diagram, but again a slight offset is observed because of the application of the Sydney Young equation. The azeotrope occurs at $x_c = 0.65$, and we note that this line on Fig. 7b is essentially a straight line with zero slope. As such, the temperature can be best represented by a mean, as was the case with ethanol + benzene and 2-propanol + benzene. Here, we find that the azeotropic temperature (corrected to standard atmospheric pressure with the Sydney Young equation) is 64.6 °C with an uncertainty of 0.2 °C. This is within the combined experimental uncertainty of the literature value of 64.7 °C [40,41].

We note that the behavior of the distillation curves is fundamentally different for this negative azeotrope than what was observed for the earlier positive azeotropes. Whereas the distillation curves for the positive azeotropes tended toward the pure components (on either side of the azeotropic point), the curves for the acetone + chloroform system show a trend toward the azeotropic composition. The mixtures with starting compositions near the azeotrope ($x_c = 0.50$, 0.70 and 0.85) show relatively flat curves with little slope, while those with starting concentrations further away from the azeotrope ($x_c = 0.05$, 010 and 0.20) show a pronounced slope. The distillations could only be carried out to the 90% distillate fractions (because of thermocouple lift out, discussed earlier), so the azeotropic composition is not actually achieved.

We can now examine the results from the composition explicit data channel, in which we have access to the dew point compositions. Sampling, analysis and standardization were performed in the same was as was done for the other two mixtures. The results of these analyses are provided in Fig. 7c. We first note that the azeotropic composition produces a flat line with zero slope, thus the composition is best represented as a mean. Our measurements indicate a composition of $x_c = 0.65$, with an uncertainty of 0.01, a value that exactly reproduces the literature value. The measured compositions of the 0.025 distillate volume fractions of $x_c = 0.05$, 0.10, 0.20, 0.50, 0.70, and 0.85 are not at the starting mole fractions of the mixtures; they are immediately shifted to the compositions of the dew point line. This is the behavior expected from the *T–x* diagram. We also note that the compositions approach the azeotropic composition from either side of the azeotrope.

The distillation curve behavior of positive and negative azeotropes is observed to be very different. While in the two examples of positive azeotropes the distillation curves approach the pure components at the anchor points very closely, the curves for the negative azeotrope do not reach the azeotropic condition, either by the temperature measurement or the composition measurement. This is especially pronounced near the azeotropic point, where the *T–x* diagram is flattened. This mirrors the extreme difficulty in the study of negative azeotropes by other VLE measurement methods resulting from the relatively small two-phase region. The azeotropic composition is usually reached only as the last film of fluid boils from the surface of the distillation flask [45–48]. In our apparatus, while we are unable to measure up to this point, rather, we can only observe the approach in both temperature and composition. Despite this limitation, we can still note the relationship with results from far more complex measurements. In mixtures where there is a large difference between the equilibrium compositions in the liquid and vapor phases, (that is, a large two-phase region sub-

Table 6
Distillation curve data (presented in °C) for binary mixtures of acetone + chloroform with starting compositions of 0.05, 0.10, 0.20, 0.50, 0.65, 0.70, and 0.85 mole fraction of chloroform (denoted as x_c in the table). In each case, the experimental pressure is provided, although the temperatures presented in the table have been adjusted with the Sydney Young equation to approximate what would be obtained at standard atmospheric pressure.

Distillate volume fraction	$x_c = 0.05$, 81.3 kPa	$x_c = 0.10$, 81.1 kPa	$x_c = 0.20$, 83.2 kPa	$x_c = 0.50$, 83.1 kPa	$x_c = 0.65$, 83.9 kPa	$x_c = 0.70$, 83.4 kPa	$x_c = 0.85$, 84.0 kPa
0.05	56.0	56.5	58.8	63.4	64.1	63.5	62.8
0.10	56.0	56.6	59.0	63.6	64.2	63.8	63.0
0.15	56.2	56.8	59.2	63.7	64.4	63.9	63.3
0.20	56.3	56.9	59.4	63.7	64.5	63.9	63.3
0.25	56.4	57.0	59.6	63.8	64.6	64.0	63.5
0.30	56.5	57.2	59.8	63.8	64.5	64.0	63.7
0.35	56.6	57.4	59.9	63.9	64.6	64.1	63.8
0.40	56.7	57.5	60.1	63.9	64.7	64.2	63.9
0.45	56.8	57.6	60.3	64.0	64.7	64.1	63.8
0.50	56.9	57.7	60.5	64.1	64.6	64.0	63.9
0.55	57.0	58.0	60.7	63.9	64.6	64.0	63.9
0.60	57.1	58.1	61.0	64.0	64.6	64.1	64.3
0.65	57.4	58.3	61.3	63.9	64.7	64.2	64.4
0.70	57.4	58.6	61.6	63.9	64.7	64.1	64.5
0.75	57.6	58.8	61.8	64.0	64.8	64.1	64.8
0.80	57.5	59.1	62.1	64.0	64.8	64.2	64.7
0.85	57.7	59.6	62.6	64.1	64.8	64.0	64.8
0.90	57.7	59.9	63.0	64.1	64.8	64.2	

tended by the bubble and dew point lines shown, for example in Fig. 5a), the composition in the boiler will change more rapidly and approach the anchor point component quickly. For mixtures with a small difference between equilibrium compositions in the liquid and vapor phases (that is, a small two-phase region subtended by the bubble and dew point lines shown, for example in Fig. 7a), the boiler composition will change slowly. For these phase diagrams, the largest changes in the compositions will occur when $(V_0 - \Delta V)$ becomes small, where V_0 is the initial volume in the kettle, and ΔV is the change in volume in the kettle [47]. The ADC method allows rapid identification of the presence of negative azeotropy. For compositions starting near the more volatile component, the distillation temperature slowly increases to temperatures above the boiling point of the more volatile component; for compositions starting near the less volatile component, the distillation temperature slowly increases to temperatures above the initial boiling point of mixture. These are indications that the mixture has a negative azeotrope.

4. Conclusions

In this paper, we have discussed how the ADC metrology can be used to detect and identify azeotropic fluid behavior (with the azeotropic inflection and convergence). We have also demonstrated that the method can be used to study the fundamentals of azeotropic phase equilibrium in a rapid and economical way, providing bubble point temperature and dew point composition information. The shapes of the distillation curves provide insight into the shapes of the corresponding *T–x* diagrams, as well as an immediate indication as to which side of the azeotrope a given mixture originates. Moreover, this shape gives an indication of the deviations from Raoult's law, with steeper curves indicating larger deviations. Both the temperature and composition channels of the ADC provide a rapid avenue to the identification of the azeotropic composition, as well as the pure component anchor points. The composition channel provides access to many other intensive properties in addition to the phase equilibrium information. These features of the ADC method provide the basis for equation of state development, as we have demonstrated elsewhere. We note that in this paper we have only studied azeotropic behavior near ambient pressure. Clearly, azeotropic behavior occurs at both higher and lower pressures. Modifications to the existing apparatus are being designed and implemented at this time to allow measurements at both higher and lower pressures.

Acknowledgments

This work was performed while ABH was supported by Summer Undergraduate Research Fellowship (SURF) award at NIST, and while LSO held a National Academy of Science/National Research Council Postdoctoral Associateship Award at NIST.

References

[1] H.Z. Kister, Distillation Operation, McGraw-Hill, New York, 1988.
[2] H.Z. Kister, Distillation Design, McGraw-Hill, New York, 1991.
[3] W. Malesinski, Azeotropy and Other Theoretical Problems of Vapor-liquid Equilibrium, Interscience, a Division of John Wiley and Sons, London, 1965.
[4] W. Swietoslawski, in: K. Ridgeway (Ed.), Azeotropy and Polyazeotropy, Macmillan Company, New York, 1963.
[5] G.M. Barrow, Physical Chemistry, McGraw-Hill College, New York, 1996.
[6] J.P. Bromberg, Physical Chemistry, Allyn and Bacon, Boston, 1984.
[7] T. Hiaki, M. Nanao, Vapor-liquid equilibria for bis (2,2,2-trifluoroethyl)ether with several organic compounds containing oxygen, Fluid Phase Equilib. 174 (1–2) (2000) 81–91.
[8] T. Hiaki, et al., Vapor-liquid equilibria for 1,1,2, 2-tetrafluoroethyl, 2,2,2-trifluoroethyl ether with several organic compounds containing oxygen, Fluid Phase Equilib 182 (1–2) (2001) 189–198.
[9] T. Hiaki, et al., Vapor-liquid equilibria for 1,1,2,3,3,3-hexafluoropropyl, 2,2,2-trifluoroethyl ether with several organic solvents, Fluid Phase Equilib 194 (2002) 969–979.
[10] S. Loras, et al., Phase equilibria for 1,1,1,2,3,4,4,5,5,5-decafluoropentane + 2-methylfuran, 2-methylfuran plus oxolane, and 1,1,1,2,3,4,4,5,5,5-decafluoropentane + 2-methylfuran plus oxolane at 35 kPa, J. Chem. Eng. Data 47 (5) (2002) 1256–1262.
[11] A. Mejia, H. Segura, M. Cartes, Vapor-liquid equilibrium, densities, and interfacial tensions for the system benzene plus propan-1-ol, Phys. Chem. Liq. 46 (2) (2008) 185–200.
[12] A. Mejia, et al., Vapor-liquid equilibrium, densities, and interfacial tensions for the system ethyl 1, 1-dimethylethyl ether (ETBE) plus propan-1-ol, Fluid Phase Equilib. 255 (2) (2007) 121–130.
[13] R.M. Villamanan, et al., Vapor-liquid equilibrium of binary and ternary mixtures containing isopropyl ether, 2-butanol, and benzene at T = 313.15 K, J. Chem. Eng. Data 51 (1) (2006) 148–152.
[14] T.J. Bruno, Improvements in the measurement of distillation curves. Part 1. A composition-explicit approach, Ind. Eng. Chem. Res. 45 (2006) 4371–4380.
[15] T.J. Bruno, B.L. Smith, Improvements in the measurement of distillation curves-part 2: application to aerospace/aviation fuels RP-1 and S-8, Ind. Eng. Chem. Res. 45 (2006) 4381–4388.
[16] T.J. Bruno, Method and apparatus for precision in-line sampling of distillate, Sep. Sci. Technol. 41 (2) (2006) 309–314.
[17] T.J. Bruno, M.L. Huber, A. Laesecke, E.W. Lemmon, R.A. Perkins, Thermochemical and thermophysical properties of JP-10, NIST-IR 6640, National Institute of Standards and Technology (U.S.A.), 2006.
[18] T.J. Bruno, Thermodynamic, transport and chemical properties of "reference" JP-8. Book of Abstracts, Army Research Office and Air Force Office of Scientific Research, 2006 Contractor's meeting in Chemical Propulsion, 2006, pp. 15–18.
[19] T.J. Bruno, The properties of S-8, Final Report for MIPR F4FBEY6237G001, Air Force Research Laboratory, 2006.
[20] T.J. Bruno, A. Laesecke, S.L. Outcalt, H.-D. Seelig, B.L. Smith, Properties of a 50/50 mixture of Jet-A + S-8, NIST-IR-6647, 2007.
[21] T.J. Bruno, B.L. Smith, Enthalpy of combustion of fuels as a function of distillate cut: application of an advanced distillation curve method, Energy Fuels 20 (2006) 2109–2116.
[22] L.S. Ott, T.J. Bruno, Corrosivity of fluids as a function of distillate cut: application of an advanced distillation curve method, Energy Fuels 21 (2007) 2778–2784.
[23] L.S. Ott, B.L. Smith, T.J. Bruno, Composition-explicit distillation curves of mixtures of diesel fuel with biomass-derived glycol ester oxygenates: a fuel design tool for decreased particulate emissions, Energy Fuels 22 (2008) 2518–2526.
[24] B.L. Smith, L.S. Ott, T.J. Bruno, Composition-explicit distillation curves of diesel fuel with glycol ether and glycol ester oxygenates: a design tool for decreased particulate emissions, Environ. Sci. Technol. 42 (20) (2008) 7682–7689.
[25] B.L. Smith, T.J. Bruno, Advanced distillation curve measurement with a model predictive temperature controller, Int. J. Thermophys. 27 (2006) 1419–1434.
[26] B.L. Smith, T.J. Bruno, Improvements in the measurement of distillation curves. Part 3. Application to gasoline and gasoline + methanol mixtures, Ind. Eng. Chem. Res. 46 (2006) 297–309.
[27] B.L. Smith, T.J. Bruno, Improvements in the measurement of distillation curves. Part 4. Application to the aviation turbine fuel Jet-A, Ind. Eng. Chem. Res. 46 (2006) 310–320.
[28] B.L. Smith, T.J. Bruno, Application of a composition-explicit distillation curve metrology to mixtures of Jet-A + synthetic Fischer-Tropsch S-8, J. Propul. Power 24 (3) (2008) 619–623.
[29] B.L. Smith, L.S. Ott, T.J. Bruno, Composition-explicit distillation curves of commercial biodiesel fuels: comparison of petroleum derived fuel with B20 and B100, Ind. Eng. Chem. Res. 47 (16) (2008) 5832–5840.
[30] E.W. Lemmon, M.O. McLinden, M.L. Huber, REFPROP, reference fluid thermodynamic and transport properties NIST Standard Reference Database 23, 2005, National Institute of Standards and Technology, Gaithersburg, MD, 2005.
[31] M.L. Huber, B.L. Smith, L.S. Ott, T.J. Bruno, Surrogate mixture model for the thermophysical properties of synthetic aviation fuel S-8: explicit application of the advanced distillation curve, Energy Fuels 22 (2008) 1104–1114.
[32] M.L. Huber, E.W. Lemmon, V. Diky, B.L. Smith, T.J. Bruno, Chemically authentic surrogate mixture model for the thermophysical properties of a coal-derived-liquid fuel, Energy Fuels 22 (2008) 3249–3257.
[33] T.J. Bruno, A. Wolk, A. Naydich, Composition-explicit distillation curves for mixtures of gasoline with four-carbon alcohols (butanols), Energy Fuels 23 (4) (2009) 2295–2306.
[34] T.J. Bruno, P.D.N. Svoronos, CRC Handbook of Basic Tables for Chemical Analysis, 2nd ed., Taylor and Francis CRC Press, Boca Raton, 2004.
[35] T.J. Bruno, P.D.N. Svoronos, CRC Handbook of Fundamental Spectroscopic Correlation Charts, Taylor and Francis CRC Press, Boca Raton, 2005.
[36] S. Young, Correction of boiling points of liquids from observed to normal pressures, Proc. Chem. Soc. 81 (1902) 777.
[37] S. Young, Fractional Distillation, Macmillan and Co., Ltd., London, 1903.
[38] S. Young, Distillation Principles and Processes, Macmillan and Co., Ltd., London, 1922.
[39] L.S. Ott, B.L. Smith, T.J. Bruno, Experimental test of the Sydney Young equation for the presentation of distillation curves, J. Chem. Thermodynam. 40 (2008) 1352–1357.
[40] J. Gmehling, J. Menke, J. Krafczk, K. Fischer, Azeotropic Data, Parts 1, 2 and 3, 2nd extended ed., Wiley VCH, Weinheim, 2004.

[41] E.W. Eashburn (Ed.), International Critical Tables (of Numerical Data, Physics Chemistry and Technology), vol. III, McGraw-Hill Book Co., 1928.
[42] R. Fritzweiler, Z. Dietrich, Der Azeotropismus und seine anwendung fur neuses verfahren sur entwasserung des aethylalkohols, Angew. Chem. 46 (1933) 241.
[43] A literature review based assessment on the impacts of a 10% and 20% ethanol gasoline fuel blend on non-automotive engines. 2002, Report to Environment Australia, Orbital Engine Company.
[44] J.M. Rhodes, T.A. Griffin, M.J. Lazzaroni, V.R. Bhenthanabotla, S.W. Campbell, Total pressure measurements for benzene with 1-propanol, 2-propanol, 1-pentanol, 3-pentanol, and 2-methyl-2-butanol at 313.15 K, Fluid Phase Equilib. 179 (2001) 217–229.
[45] C.D. Holcomb, National Institute of Standards and Technology, retired. 2008.
[46] J.R. Noles, J.A. Zollweg, Isothermal vapor liquid equilibrium for dimethyl ether + sulfur dioxide, Fluid Phase Equilib. 66 (3) (1991) 275–289.
[47] J.R. Noles, Vapor liquid equilibria of solvating binary mixtures, Department of Chemical Engineering, Cornell University, Ithica, 1991, p. 273.
[48] J.R. Noles, J.A. Zollweg, Vapor-liquid equilibrium for chlorodifluoromethane + dimethyl ether from 283 to 395 K at pressures to 5.0 MPa, J. Chem. Eng. Data 37 (3) (1992) 306–310.